NIPP1 maintains EZH2 phosphorylation and promoter occupancy at proliferation-related target genes

Nikki Minnebo[1], Janina Görnemann[1], Nichole O'Connell[3], Nele Van Dessel[1], Rita Derua[2], Marit Willemijn Vermunt[1], Rebecca Page[4], Monique Beullens[1], Wolfgang Peti[3,5], Aleyde Van Eynde[1] and Mathieu Bollen[1]

[1]Laboratory of Biosignaling & Therapeutics, Department of Cellular and Molecular Medicine, Faculty of Medicine, KU Leuven, B-3000 Leuven, Belgium;

[2]Laboratory of Protein Phosphorylation and Proteomics, Department of Cellular and Molecular Medicine, Faculty of Medicine, KU Leuven, B-3000 Leuven, Belgium.

[3]Department of Molecular Pharmacology, Physiology and Biotechnology, Brown University, Providence, RI, USA;

[4]Department of Molecular Biology, Cell Biology and Biochemistry, Brown University, Providence, RI, USA;

[5]Department of Chemistry, Brown University, Providence, RI, USA.

Inventory

This file contains 8 supplementary figures and 1 supplementary table.

SUPPLEMENTARY DATA

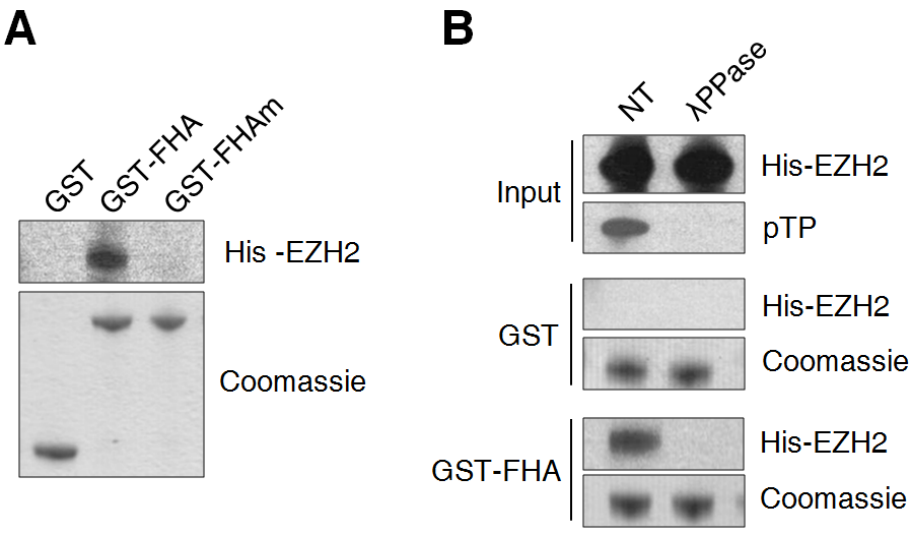

Figure S1. Determinants of the NIPP1-EZH2 interaction. (**A**) GST pull-down assays were performed after incubation of baculovirus-expressed His-EZH2 with GST-FHA, GST-FHAm or GST as a control. (**B**) Same as in (**A**) after incubation of His-EZH2 with phosphatase inhibitors (NT) or lambda phosphatase (λPPase). The dephosphorylation of His-EZH2 was verified by immunoblotting with pan-pTP antibodies.

A

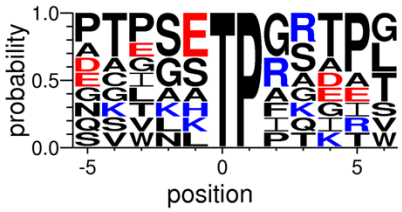

B

	TP1	TP2	TP3	TP4	TP5	TP6
H. sapiens	LPPECTPNIDGP	HPFHATPNTYKR	AERIKTPPKRPG	SSRPSTPTINVL	NSRCQTPIKMKP	AEDVDTPPRKKK
M. musculus	LPPECTPNIDGP	HPFHATPNTYKR	AERIKTPPKRPG	SSRPSTPTISVL	NSRCQTPIKMKP	TEDVDTPPRKKK
G. gallus	LPPECTPNIDGP	HPFHATPNTYKR	AERIKTPPKRPG	TSRPSTPTINVL	NSRCQTPIKMKP	AEDVDTPPRKKK
D. rerio	LPPECTPNIDGP	HPFHATPNTYKR	PERAKTPSKRST	NSRPSTPTVNS-	NSRCQTPVKLKL	AVDENTPQRKKK

Figure S2. The NIPP1 FHA domain preferentially binds phosphorylated Thr-Pro motifs. (**A**) Sequence binding preference of known NIPP1 FHA ligands (MELK, CtIP, CDC5L, and SAP155), as predicted by Weblogo (40). (**B**) Conservation of the six TP-dipeptide motifs of EZH2 between species.

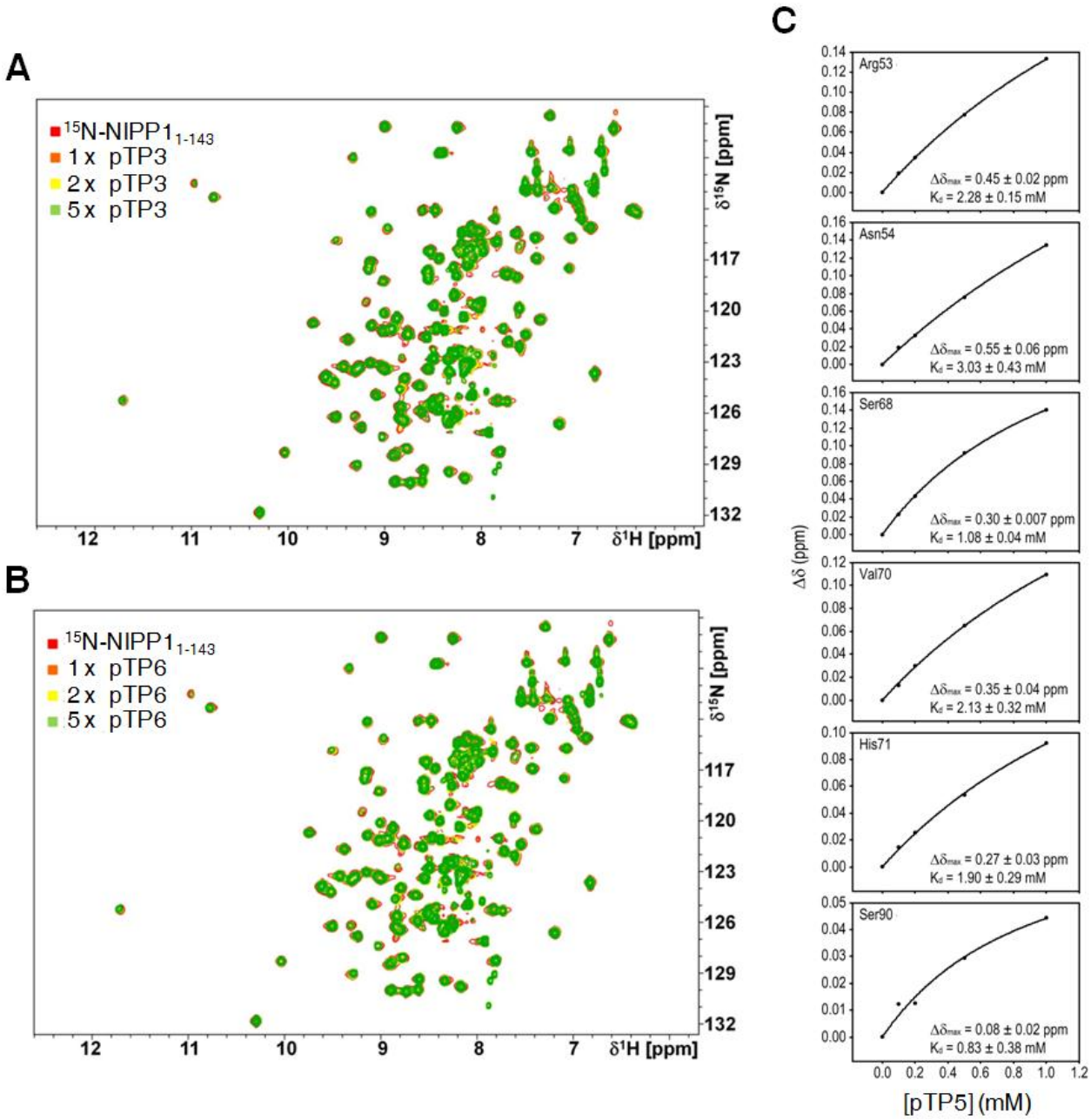

Figure S3. NMR studies of the interaction of EZH2-derived phosphopeptides with NIPP1-FHA. (**A**) 2D [^{1}H,^{15}N] HSQC spectrum of the ^{15}N-labeled NIPP1-FHA (red), and different ratios of FHA:pEZH2$^{339-351}$; 1:1 (orange), 1:2 (yellow) and 1:5 (green). No chemical shift perturbations are detected. (**B**) 2D [^{1}H,^{15}N] HSQC spectrum of ^{15}N-labeled NIPP1-FHA (red), and different ratios of FHA:pEZH2$^{483-495}$; 1:1 (orange), 1:2 (yellow) and 1:5 (green). No chemical shift perturbations are detected. (**C**) CSP vs concentration analysis of NIPP1 residues Arg53, Asn54, Ser68, Val70, His71 and Ser90 to calculate a lower boundary of the K_d for pTP5 peptide binding.

A

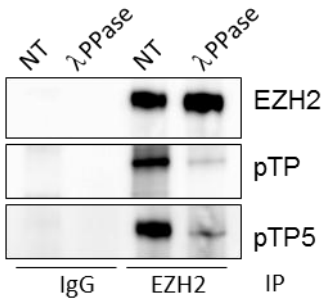

B

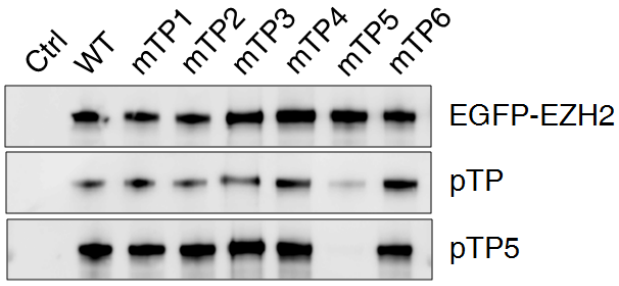

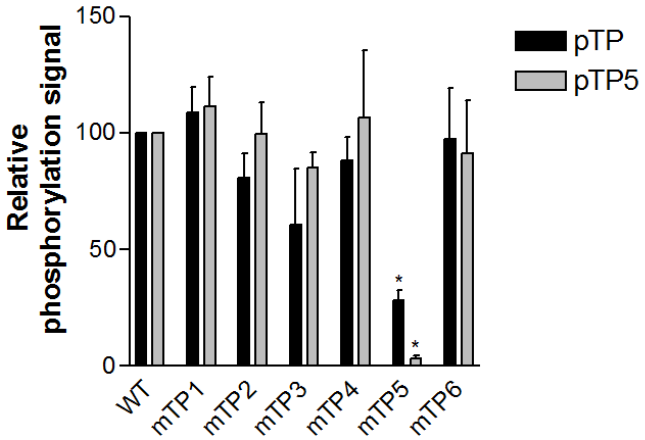

Figure S4. Endogenous chromatin-associated EZH2 and ectopically expressed EGFP-EZH2 are phosphorylated at TP-dipeptides and TP5. (**A)** Endogenous EZH2 was immunoprecipitated from the chromatin-enriched fraction of a HEK293T cell lysate. The lysate was pre-incubated with phosphatase inhibitors (NT) or with lambda phosphatase (λPPase). The phosphorylation status of EZH2 was verified by immunoblotting with pan-TP and phospho-TP5 specific antibodies. (**B**) Ectopically expressed EGFP-EZH2 is phosphorylated at TP-dipeptides and TP5, and a NIPP1-binding mutant of EZH2 is hypophosphorylated on TP-motifs. EGFP (Ctrl) or EGFP-EZH2 (WT or indicated Thr to Ala mutants) were EGFP-trapped and their phosphorylation was analyzed by immunoblotting with pan-pTP and pTP5 antibodies. The lower panel shows the means ± SEM for 3 experiments. (* $p<0.01$; paired Student's *t*-test).

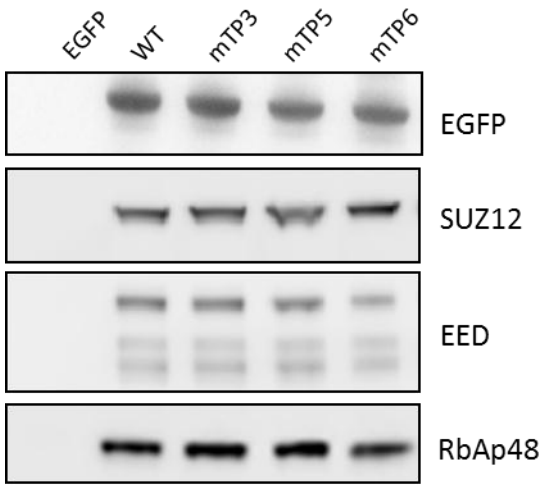

Figure S5. The Ala mutation of Thr345 (TP3), Thr416 (TP5) and Thr487 (TP6) of EZH2 does not affect the integrity of the PRC2 core complex. Ectopically expressed EGFP or EGFP-tagged EZH2-WT, EZH2-mTP3, EZH2-mTP5 or EZH2-mTP6 were immunoprecipitated from HEK293T cell lysates using EGFP-trap, and analysed for co-immunoprecipitation of the PRC2 components SUZ12, EED and RbAp48.

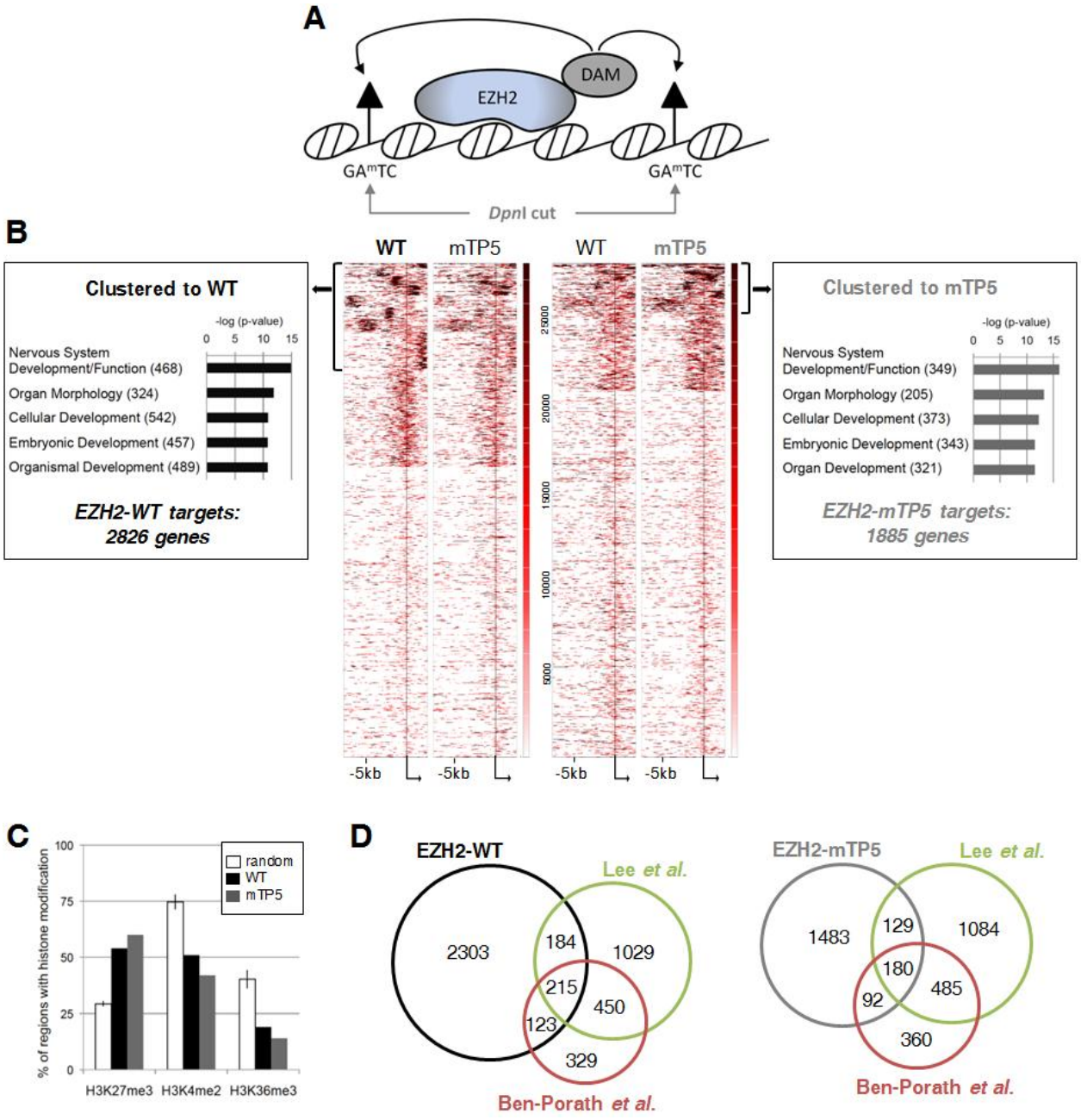

Figure S6. Mapping of the promoter-binding sites of EZH2-WT and EZH2-mTP5. (**A**) Scheme illustrating how the chromatin targeting of EZH2-Dam results in local DNA methylation at GATC sequences, thus creating a restriction site for *Dpn*I. (**B**) Heatmap clustering reveals enriched binding sites relative to transcription start sites. Bigwig files were clustered (k-means 10) in relation to genome-wide transcription start sites for the -7.5kb to +2.5kb region using the cistrome tool. Center left: Clustering according to EZH2-WT signal, center right: clustering according to EZH2-mTP5 signal. Enlargement

of the most prominent clusters is shown to the left (WT) and right (mTP5). Clusters overlap to a certain extent between the two datasets, but the mTP5 data set results in smaller clusters. Clustering was performed four times independently and the genes represented by the prominent clusters were identified. The intersection of the four gene collections resulted in a set of 2826 genes (EZH2-WT) and 1885 genes (EZH2-mTP5) respectively, which were found in clusters consistently. These target genes were subjected to IPA analysis confirming their involvement in developmental processes. (**C**) Histone modifications show an enrichment of H3K27me3. The -4kb to +4kb window around the TSS of three random gene lists (each containing around 1440 TSS; white bars), the EZH2 WT (black) and mTP5 (grey) target gene lists were analyzed for the presence of the H3K27me3, H3K4me2 and H3K36me3 histone modifications, based on the data specific for HeLa cells available through the UCSC genome website. The plot shows the percentage of regions with the respective modification in relation to the complete set of regions. The white bars represent the average of the three random TSS sets with error bars indicating SD. (**D**) Overlap between the EZH2 WT and mTP5 target gene lists determined by DamID in HeLa cells and previously published lists for SUZ12 associated genes (33*)* and H3K27me3 (32) in human ES cells.

A

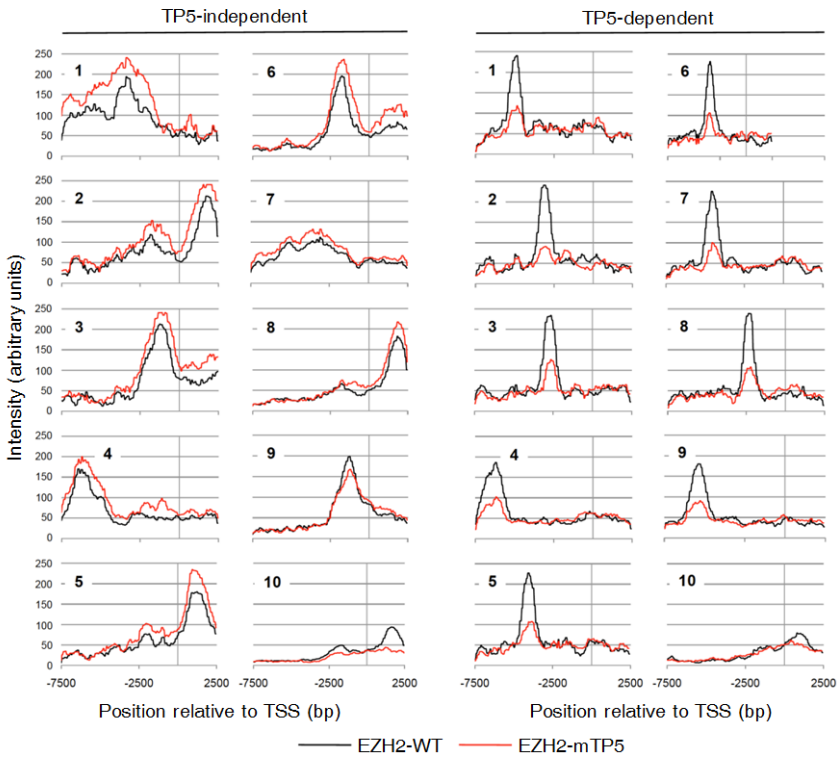

B.

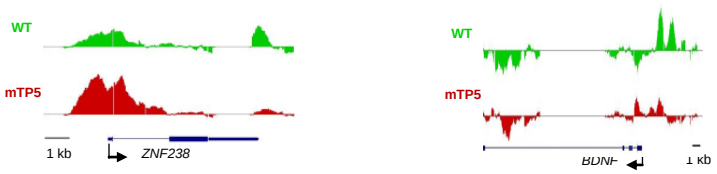

Figure S7. NIPP1 regulates EZH2 association and mRNA expression at "TP5-dependent" target genes. (**A**) Density plots across each cluster derived from Figure 4B using ImageJ. (**B**) DamID-binding profiles of EZH2 at the indicated genes. *ZNF238* belongs to cluster 4 of TP5-independent genes and *BDNF* to cluster 10 of TP5-dependent genes.

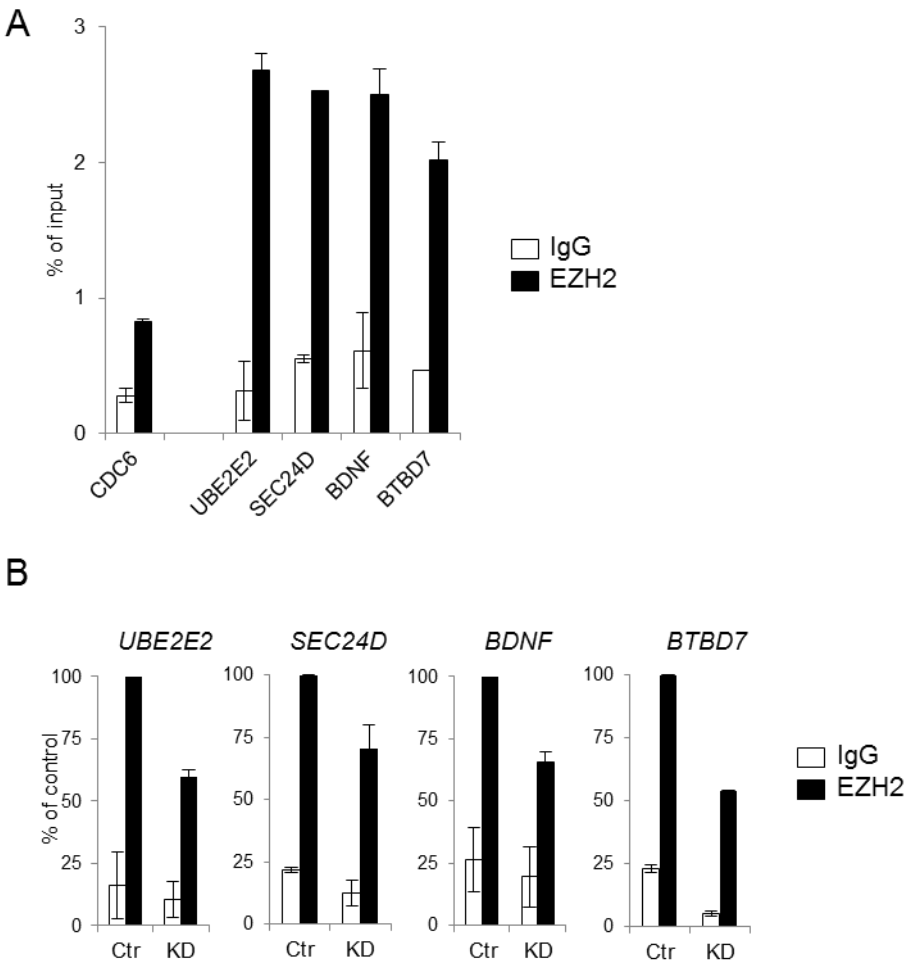

Figure S8. The downregulation of NIPP1 is associated with a deficient binding of EZH2 to TP5-dependent target genes. ChIPs were performed using antibodies against EZH2 (black bars) in HeLa cells treated with control (Ctr) or NIPP1 (KD) siRNAs and analysed for the indicated genes. ChIPs with IgGs served as negative controls (white bars) and *CDC6* was used as a non-target gene. ChIP enrichments (n = 2-3 independent ChIP experiments) are expressed as a percentage ± SEM of the total input signal (A) or as a percentage ± SEM of the data obtained with the control siRNA (B).

Table S1. HeLa target gene lists of EZH2-WT and EZH2-mTP5, as determined by DamID. *Table S1 is provided as a separate Excel data-sheet.*

SUPPLEMENTARY REFERENCE

41. Crooks,G.E., Hon,G., Chandonia,J.M. and Brenner,S.E. (2004) WebLogo: a sequence logo generator. *Genome Res.*, **14**, 1188-1190.